


# Design and Analysis of Compliant Rack and Pinion Using Compliant Contact Rolling Joint <sup>†</sup>

Lakshmipathy Panchanathan and Shyh-Chour Huang \* 

Department of Mechanical Engineering, National Kaohsiung University of Science and Technology, Kaohsiung 807618, Taiwan; lakshmipathy351@gmail.com

\* Correspondence: shuang@nkust.edu.tw

<sup>†</sup> Presented at the 3rd IEEE International Conference on Electronic Communications, Internet of Things and Big Data Conference 2023, Taichung, Taiwan, 14–16 April 2023.

**Abstract:** This paper presents the design of a compliant rack and pinion mechanism with the support of a compliant rolling contact joint (CRCJ). The flexible strips are mounted to connect the rack and pinion to accelerate the mechanism. Two types of rack and pinion mechanism are proposed: rack and pinion mechanism and double rack and pinion actuator. The 3D model is created with finite element analysis (FEM) for structural analysis to observe the maximum strength and the deformation of the flexible strip. A 3D-printed model is proposed by using a fused deposition method (FDM) by printing layer by layer for experimental and demonstration purposes. In this study, we propose a set of examples to convert a traditional rigid body mechanism to complete a complaint mechanism to accumulate the actual function and also to increase the high possibilities of mounting.

**Keywords:** compliant mechanism; rack and pinion mechanism; compliant contact rolling joint; rack and pinion actuator

## 1. Introduction

The rack and pinion mechanism is the traditional mechanism to convert rotational motion into linear motion. By bearing the pinion, we transform line motion to rotational motion [1,2]. Rack and pinion is a well-known steering mechanism. A pinion is attached to the end of the steering shaft in the rack and pinion type of steering mechanism. Because the pinion and the rack are mated, the movement of the handle causes the pinion to rotate, which in turn causes the rack to move sideways. Another application of rack and pinion is actuators, which contain dual racks and single pinions. In pipeline transport, valve control is accomplished with pneumatic rack and pinion actuators [3].

The compliant mechanism holds the potential for flexibility. The mobility of the compliant mechanism at least gains from the deflection of flexible members rather than from movable joints only [4]. This design is inspired by the compliant rolling contact joint (CRCJ) mechanism [5,6]. The conventional CRCJ consists of four similar semi-cylindrical cams connected in a row at alternative positions, as shown in Figure 1. The flexure straps deform until both cams are aligned and connected [7,8]. To achieve zero angular stiffness, the compliant rolling contact joint has maintained the strain energy at a constant level while in action [9,10].

We introduce two compliant rack and pinion mechanisms: a rack and pinion steering mechanism and a rack and pinion actuator. With the knowledge of compliant rolling, the design of the mechanism is proposed. The vivid functions of steering and actuator mechanisms are presented in this study. The following design is created with FEM for structural analysis.



**Citation:** Panchanathan, L.; Huang, S.-C. Design and Analysis of Compliant Rack and Pinion Using Compliant Contact Rolling Joint. *Eng. Proc.* **2023**, *38*, 36. <https://doi.org/10.3390/engproc2023038036>

Academic Editors: Teen-Hang Meen, Hsin-Hung Lin and Cheng-Fu Yang

Published: 26 June 2023



**Copyright:** © 2023 by the authors. Licensee MDPI, Basel, Switzerland. This article is an open access article distributed under the terms and conditions of the Creative Commons Attribution (CC BY) license (<https://creativecommons.org/licenses/by/4.0/>).



Figure 1. Core [4].

## 2. Design and Fabrication

### 2.1. Design and Modeling

The model was designed by using Solidworks. Figure 2 represents the components of the pinion, rack, flexible strip, and casing. The pinion was designed with four pairs of grooves, shafts, and pivotal holes. The extrusion of the rib around the pinion (1 mm) was placed in the center of the pinion, as shown in Figure 2a. The rack contained four grooves, and the slot was designed in the middle of the rack, as shown in Figure 2b. In Figure 2c, the flexible strip was designed according to the circumference of the pinion. The geometry of the flexible strip was designed to place in-between pinion and rack grooves. The casing was modeled to mount all the parts inside. To prevent slippage during running, 2 pathways were presented to mount the rack and for the sliding motion, as shown in Figure 2d. The dimensions of all the components are shown in Table 1.

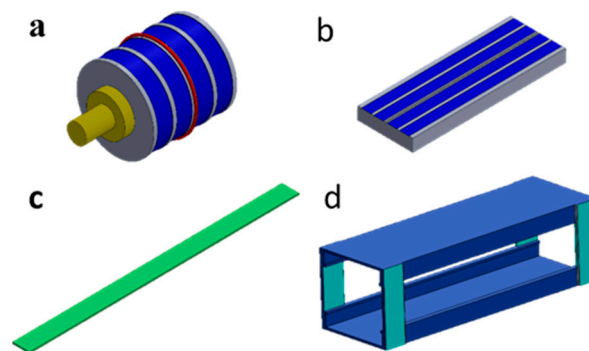


Figure 2. Model of components: (a) pinion; (b) rack; (c) flexible strip; (d) casing.

Table 1. Dimensions of the components.

Objects	Length	Thickness	Diameter
Pinion	43 mm	-	40 mm
Rack	125 mm	10 mm	-
Flexible strip	125 mm	0.6 mm	-
Casing	160 mm	64 mm	-

The flexible strip was modeled according to the circumference of the pinion. The radius of the pinion  $R$  was 20 mm. The perimeter of the circle is denoted as,

$$C = 2\pi R \text{ or } \pi D \quad (1)$$

The total length of the flexible strip was 125 mm, and the length of the flexible strip and the circumference of the pinion were relative to each other when the pinion diameter was increased as the total length of the flexible strip also increased.

The CRCJ mechanism is constrained by the contact surface to have a constant curvature. This constant curvature creates well-defined moments in the flexures. The relationship between the curvature of a beam and the internal moments is defined by the Bernoulli–Euler equation.

$$M = EI \frac{d\theta}{ds} \quad (2)$$

where  $E$  is the modulus of elasticity,  $I$  is the moment of inertia, and  $d\theta/ds$  is the curvature.

The Bernoulli–Euler equation is valid for large deflections. The beam with a constant radius of curvature creates a moment that is also constant along the beam length. This means the segment has the same behavior as a beam with a moment applied to the free end.

$$M = \frac{EI}{R'} \quad (3)$$

Thus, the maximum stress in the CRCJ depends on the modulus of elasticity of the chosen material, the thickness of the flexure, and the effective radius of curvature [4,11].

## 2.2. Manufacturing

The parts were manufactured with polylactic acid (PLA) material. The FDM method was used for the 3D models, which were printed layer-by-layer using thermoplastic filaments to create the 3D-printed model. After the development of the model, the model is exported into Ultimaker Cura 5.1, Taipei, Taiwan. the slicing process was done by Cura 5.1. The infill rate was 100%, the printing temperature of the PLA material was 220 °C, and the bed temperature was 200 °C. Then, the file is transferred to JGmaker 3d printing machine, Taipei, Taiwan for fused deposition method (FDM) layer-by-layer printing. The material used for simulation was polylactic acid (PLA) with a density of 1.28 g/cm<sup>3</sup>, Young's modulus was 2.7 GPa, and tensile strength was 62.9 MPa.

## 3. Results

### 3.1. Pinion

Normally, the rolling contact joint mechanism is considered to be a semi-cylindrical type. The movement we obtained was less than 180°. The rotation occurred at half of the circumference. The compliant pinion played a vital role in this design to obtain the maximum linear motion. We achieved the maximum circumference of the pinion rotation with the help of compliant flexible strips.

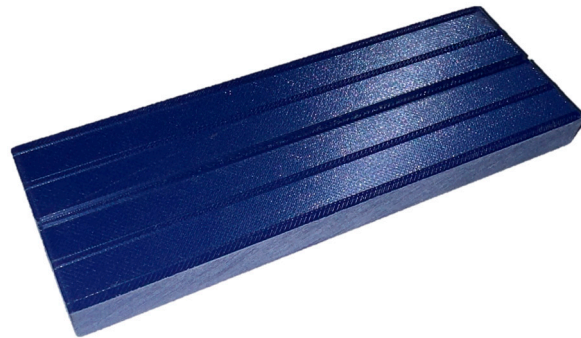
The compliant pinion contained four grooves (0.4 mm), and in the center, an extruded part was placed to prevent pinion slippage, as shown in Figure 3. To actuate the pinion, two types of input and output methods were designed. For shafts and holes, we obtained the linear motion by actuating the rack and the placement of the bearing into the hole to achieve the linear rotation motion.



Figure 3. Pinion.

### 3.2. Compliant Rack

The compliant rack had the same grooves in the pinion; the groove depth of the compliant rack was 0.2 mm. The center groove was presented to mount the pinion in that precise groove to avoid slippage, as shown in Figure 4. The rolling compliant contact joint had two types of cylinder parts placed opposite to each other, but the grooves were placed on either side of the cylinder part. We increased the efficiency of the design; the grooves in the rack were placed to minimize the strain on the flexible strip. The pinion rotated in two directions: clockwise and counterclockwise. While in the clockwise direction, the rack moved forward; in the counterclockwise direction, a backward linear motion was observed.



**Figure 4.** Rack.

### 3.3. Flexible Strip

The flexible strips play a vital role in this design. The rack and pinion had four grooves placed on each other. The rack had 0.2 mm grooves, and the pinion had 0.4 mm grooves. The total thickness of the flexible strip was 0.6 mm, as shown in Figure 5. Four strips were connected to the grooves to operate the rack and pinion. The two strips were connected in the clockwise grooves to make the clockwise and forward motion of the compliant rack and pinion. The other two strips were connected in the center or counterclockwise grooves of the compliant rack and pinion to make the backward linear motion. By altering the positions of the flexible strips, we created two types of mechanism, a steering rack and pinion mechanism and a rack and pinion actuator.

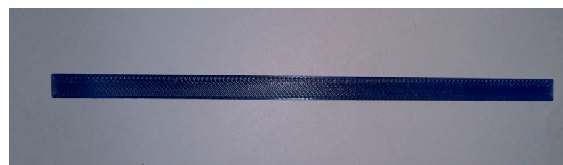


**Figure 5.** Flexible strip.

The pair of the rack was actuated by pinion with the help of compressed air to obtain the clockwise and the anti-clockwise motion. The placement of both clockwise and counterclockwise strips in the bottom of the rack achieved the steering rack and pinion mechanism. Placing the clockwise strips at the bottom of the rack and the counterclockwise strip at the top of the rack with the support of the casing achieved the rack and pinion actuator.

### 3.4. Casing

The pinion, rack, and flexible strips were mounted into the casing. The casing covered all the parts and prevented slippages during the working condition, as shown in Figure 6. To obtain the changes in the steering and actuator rack and pinion mechanism, the rack and the flexible strip placement were different in the mounting positions. The rack was positioned inside the casing ribs so that the rack moved independently. To obtain the steering rack and pinion mechanism, both racks were connected, and the flexible strips were mounted on the bottom of the rack.



**Figure 6.** Casing.

The actuation of the pinion moved the bottom rack and the supporting rack to linear motion. For the rack and pinion actuator, the top rack and the bottom rack moved independently to acquire the parallel forward and backward motion. The clockwise flexible strips were connected to the bottom of the rack, and the counterclockwise strips were connected to the top of the rack to achieve the mechanism by the support of the casing.

### *3.5. Rack and Pinion Steering Mechanism*

The assembled view of the compliant rack and pinion mechanism is presented in Figures 7 and 8. Figure 7 represents the isometric view of the rack and pinion mechanism. The casing contains a slot to hold the top and base rack for sliding motive. The pinion is placed in between both racks. The flexible strips play a vital role in connecting the rack and pinion for the motions. Four grooves are made in the rack and pinion; a pair of grooves represent clockwise grooves placed on both ends, and a further pair denotes counterclockwise grooves located center. The base rack and the pinion are connected by two flexible strips in clockwise grooves, and the other pair of flexible strips connect the base rack and pinion in counter-clockwise grooves. For the first type of rack and pinion mechanism, both racks are connected by a supporting plate to obtain the parallel line motion. Actuating the base rack leads a way to act together. The counterclockwise rotation of the pinion assists the base rack in moving forward with the help of flexible strips connected in the counterclockwise grooves. The clockwise rotation motion of the pinion tends to move the rack backward in linear motion by the guidance of a flexible strip connected in the clockwise grooves. By bearing the pinion, giving the liner input to the racks allows the output of rotational motion.

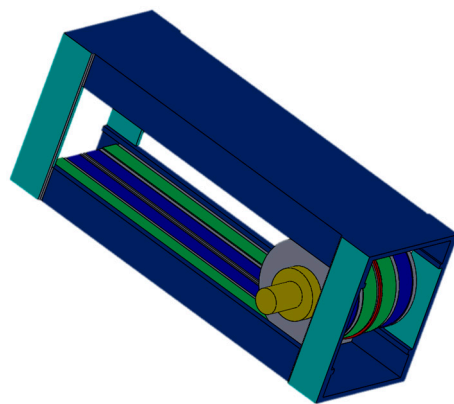


**Figure 7.** Isometric view of rack and pinion mechanism.

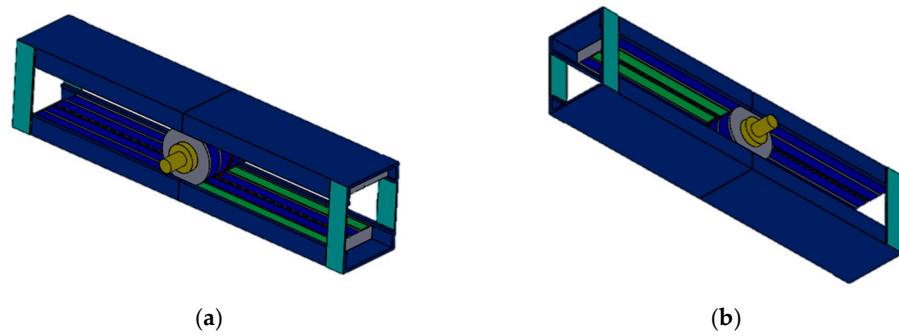


**Figure 8.** Isometric view of the double rack and pinion actuator: (a) base rack; (b) top rack.

### 3.6. Rack and Pinion Actuator

Figure 8 represents the design of the rack and pinion actuator and the placement of the flexible strip and the rack in the actuator mechanism. The base rack holds the position at the bottom of the casing as well as the top rack in the top slot of the casing. The pair of flexible strips connect the pinion and the base rack at the clockwise grooves, as denoted in Figure 9. The second pair of flexible strips connect the top rack and the pinion in counterclockwise grooves, as represented in Figure 9. The clockwise motion of the pinion makes the base rack move backward, and the top rack moves forward. The counterclockwise motion leads a base rack to move forward and the top rack to slide backward. By pivoting the pinion and the input of the rack, linear motion turns into rotational motion.

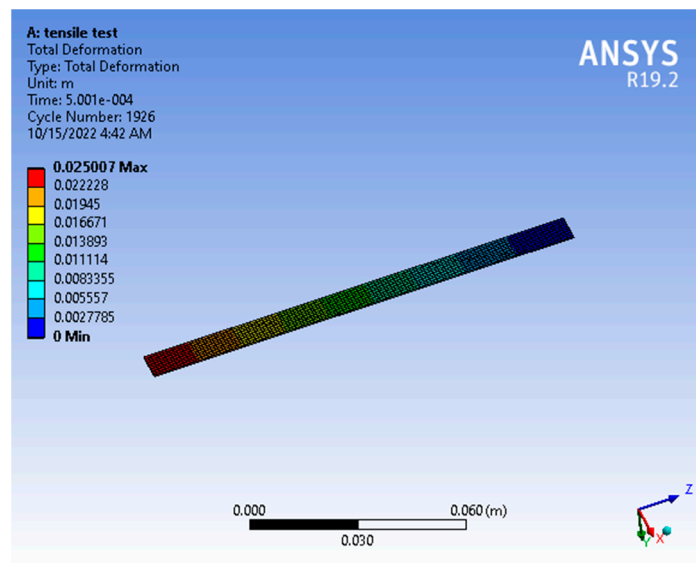


**Figure 9.** Total deformation.

### 3.7. Finite Element Analysis

The finite element method (FEM) was conducted using ANSYS. The maximum torque of the pinion and the load increment of the rack increases the tension of the flexible cable [12]. The FEM was used to figure out the maximum stress and deformation of the flexible strips. Figure 9 presents the computation of total deformation and the maximum deformation of the flexible strip of 0.025 mm. The plot of maximum deformation is shown in Figure 10. The material deformation occurs in the fixed position of the rack. When converting the linear motion into rotational motion, the load is applied to the rack. The flexible strip connects the rack and pinion. The rack is subjected to the maximum load, and the stress also increases in the flexible strip. However, the compressive force acting on the flexible strip reduces the tension occurrence. The stress is induced by the flexible cable. To observe the stress activity of the flexible strip, von-mises stress was exerted. The maximum



stress of the flexible strip is  $4.4593 \times 10^8$  Pa, and the value of minimum stress obtained at  $2.8991 \times 10^8$  Pa is shown in Figures 11 and 12.

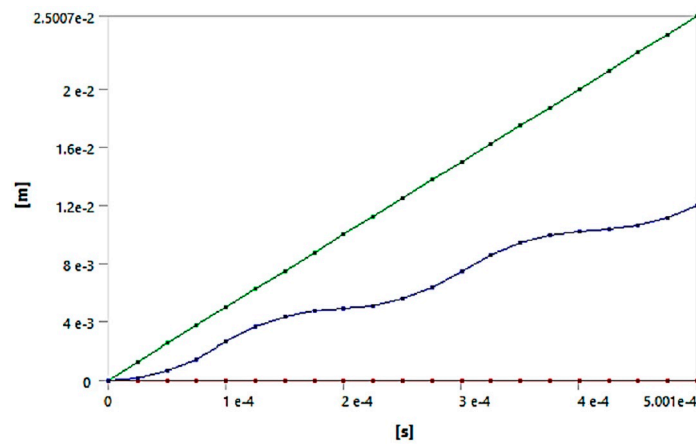


Figure 10. FEA Total deformation.

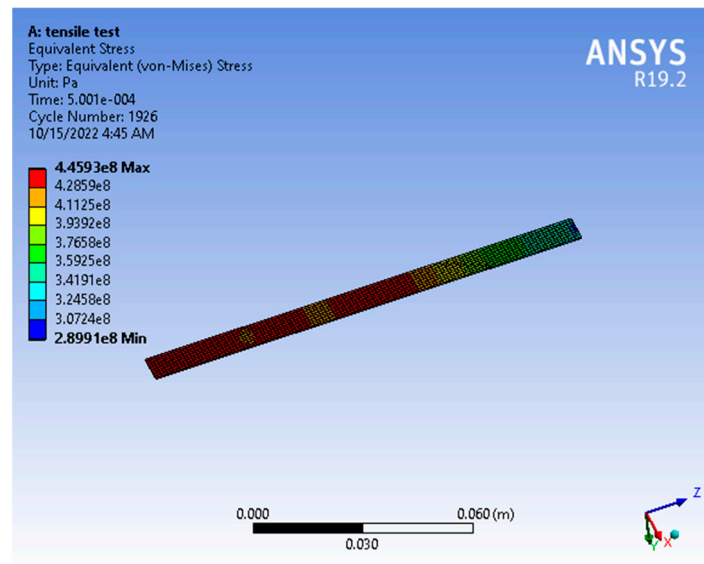


Figure 11. Von-mises stress.

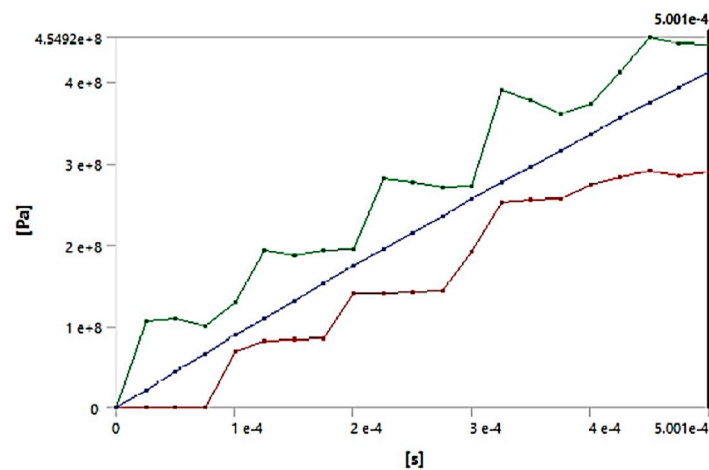


Figure 12. FEA Equivalent (von-mises).

#### 4. Discussion

For the replacement of the traditional rack and pinion method, a novel method was developed to achieve the respective motions. The compliant rolling contact joint (CRCJ) is the major inspiration for this model. The CRCJ joint acts as a gear. Instead of the gear teeth, the flexible strips are connected as two rigid links to keep no-slip contact. The flexure avoids being stretched or becoming loose. Further, it achieves zero angular stiffness to maintain a constant level of strain energy in rotation. However, the conditions are impossible for the CRCJ joint to achieve the 360° full rotation, as the internal stress does not increase. To obtain the total length of the rack movement, the pinion approximately rotates less than (>360°), acquiring the internal stress and maintaining the constant strain energy. The position of the flexible strip in between the rack and pinion grooves reduces the flexible strip tension.

#### 5. Conclusions

We presented the two types of compliant rack and pinion methods. The movement of linear motion depends on the circumference of the pinion of 40 mm in diameter. The total length of linear motion is 125 mm. This method is inspired by CRCJ, and the rotation motion of the pinion is >360°. The maximum deformation is 0.025 mm, and the maximum stress of flexible cable is  $4.4593 \times 108$  Pa. The design successfully achieves linear motion as well as rotational motion by using the flexible component. The speed of the motions increases with the traditional rack and pinion mechanism. In the future, the movement of the rack needs to increase using the threading technique. For example, the total length of linear motion depends on the circumference of the pinion. By introducing the threading technique, the pinion achieves twice the linear motion.

**Author Contributions:** Conceptualization, S.-C.H.; methodology, S.-C.H.; software, L.P.; validation, L.P. and S.-C.H.; formal analysis, L.P.; writing—original draft preparation, L.P.; writing—review and editing, S.-C.H. All authors have read and agreed to the published version of the manuscript.

**Funding:** This research received no external funding.

**Institutional Review Board Statement:** Not applicable.

**Informed Consent Statement:** Not applicable.

**Data Availability Statement:** Not applicable.

**Acknowledgments:** The authors acknowledge and thank the Ministry of Science and Technology of the Republic of China for their partial financial support of this study under Contract Number MOST 111-2221-E-992-068.

**Conflicts of Interest:** The authors declare no conflict of interest.

#### References

1. Torvi, S.; Ingale, V.; E, R.K. Design and Analysis of Rack and Pinion Mechanism in Automobile Applications Using Structural Steel and PLA. *Int. J. Prod. Eng.* **2018**, *4*, 13–22. [[CrossRef](#)]
2. Akash, K.; Sangavi, S.; Venkatesan, M. Double acting syringe pump using a rack and pinion mechanism—Simulink model. In Proceedings of the 2016 IEEE International Conference on Computational Intelligence and Computing Research (ICIC), Tamil Nadu, India, 15–17 December 2016; pp. 1–4.
3. Mustalahti, P.; Mattila, J. Nonlinear model-based controller design for a hydraulic rack and pinion gear actuator. In *Fluid Power Systems Technology*; American Society of Mechanical Engineers: New York, NY, USA, 2018; Volume 51968, p. V001T01A020.
4. Cannon, J.R.; Craig, P.L.; Larry, L.H. Compliant rolling-contact element mechanisms. In Proceedings of the International Design Engineering Technical Conferences and Computers and Information in Engineering Conference, Long Beach, CA, USA, 24–28 September 2005; Volume 47446, pp. 3–13.
5. Zhang, D.; Sun, Y.; Lueth, T.C. Design of a novel tendon-driven manipulator structure based on monolithic compliant rolling-contact joint for minimally invasive surgery. *Int. J. Comput. Assist. Radiol. Surg.* **2021**, *16*, 1615–1625. [[CrossRef](#)] [[PubMed](#)]
6. Hu, Y.; Zhang, L.; Li, W.; Yang, G.-Z. Design and Fabrication of a 3-D Printed Metallic Flexible Joint for Snake-Like Surgical Robot. *IEEE Robot. Autom. Lett.* **2019**, *4*, 1557–1563. [[CrossRef](#)]



7. Shaw, L.A.; Chizari, S.; Dotson, M.; Song, Y.; Hopkins, J.B. Compliant rolling-contact architected materials for shape reconfigurability. *Nat. Commun.* **2018**, *9*, 4594. [[CrossRef](#)] [[PubMed](#)]
8. Kim, S.-H.; Hyunki, I.; Song, J.-R.; Cho, K.-J. Force characteristics of rolling contact joint for compact structure. In Proceedings of the 2016 6th IEEE International Conference on Biomedical Robotics and Biomechatronics (BioRob), Singapore, 26–29 June 2016; pp. 1207–1212.
9. Nelson, T.G.; Lang, R.J.; Magleby, S.P.; Howell, L.L. Curved-folding-inspired deployable compliant rolling-contact element (D-CORE). *Mech. Mach. Theory* **2016**, *96*, 225–238. [[CrossRef](#)]
10. Jeanneau, A.; Herder, J.; Laliberté, T.; Gosselin, C. A compliant rolling contact joint and its application in a 3-dof planar parallel mechanism with kinematic analysis. In Proceedings of the International Design Engineering Technical Conferences and Computers and Information in Engineering Conference, Salt Lake City, UT, USA, 28 September–2 October 2004; Volume 46954, pp. 689–698.
11. Halverson, P.A.; Howell, L.L.; Jensen, B.D.; Magleby, S.P. Concepts for achieving multi-stability in compliant rolling-contact elements. In Proceedings of the International Design Engineering Technical Conferences and Computers and Information in Engineering Conference, Las Vegas, NV, USA, 4–7 September 2007; Volume 48094, pp. 67–73.
12. Halverson, P.A.; Howell, L.L.; Magleby, S.P. Tension-based multi-stable compliant rolling-contact elements. *Mech. Mach. Theory* **2010**, *45*, 147–156. [[CrossRef](#)]

**Disclaimer/Publisher’s Note:** The statements, opinions and data contained in all publications are solely those of the individual author(s) and contributor(s) and not of MDPI and/or the editor(s). MDPI and/or the editor(s) disclaim responsibility for any injury to people or property resulting from any ideas, methods, instructions or products referred to in the content.